OFFICE OF NAVAL RESEARCH

Contract N00014-87-K-0494

R&T Code 400X027YIP

Technical Report No. 10

Nonlocal Free Energy Density Functional Approximations for the Electrical Double Layer; Comparison with Monte Carlo Results for 2:1 Salts

by

L. Miery-y-Teran, Zixiang Tang, H.S. White, and H.T. Davis

Prepared for Publication in the

Journal of Chemical Physics

University of Minnesota
Department of Chemical Engineering and Materials Science
Minneapolis, MN 55455

April 10, 1990

SECURITY CLASSIFICATION OF THIS PAGE

REPORT DOCUMENTATION PAGE

1a. REPORT SECURITY CLASSIFICATION Unclassified	1b. RESTRICTIVE MARKINGS
2a. SECURITY CLASSIFICATION AUTHORITY	3. DISTRIBUTION/AVAILABILITY OF REPORT
2b. DECLASSIFICATION/DOWNGRADING SCHEDULE	Unclassified/Unlimited
4. PERFORMING ORGANIZATION REPORT NUMBER(S) ONR Technical Report 10	5. MONITORING ORGANIZATION REPORT NUMBER(S)
6a. NAME OF PERFORMING ORGANIZATION Dept of Chemical Engineering and Materials Science 6b. OFFICE SYMBOL (If applicable) Code 1113	7a. NAME OF MONITORING ORGANIZATION Office of Naval Research
6c. ADDRESS (City, State, and ZIP Code) University of Minnesota Minneapolis, MN 55455	7b. ADDRESS (City, State, and ZIP Code) 800 North Quincy Street Arlington, VA 22217
8a. NAME OF FUNDING/SPONSORING ORGANIZATION Office of Naval Research 8b. OFFICE SYMBOL (If applicable)	9. PROCUREMENT INSTRUMENT IDENTIFICATION NUMBER Contract No. N00014-87-K-0494
8c. ADDRESS (City, State, and ZIP Code) 800 North Quincy Street Arlington, VA 22217-5000	10. SOURCE OF FUNDING NUMBERS PROGRAM ELEMENT NO. / PROJECT NO. / TASK NO. / WORK UNIT ACCESSION NO

11. TITLE (Include Security Classification)
Nonlocal Free Energy Density Functional Approximations for the Electrical Double Layer, Comparison with Monte Carlo Results for 2:1 Salts

12. PERSONAL AUTHOR(S)
L. Miery-y-Teran, Zixiang Tang, H.S. White and H.T. Davis

13a. TYPE OF REPORT	13b. TIME COVERED	14. DATE OF REPORT (Year, Month, Day)	15. PAGE COUNT
Technical	FROM _____ TO _____		

16. SUPPLEMENTARY NOTATION
prepared for publication in the Journal of Chemical Physics

17. COSATI CODES			18. SUBJECT TERMS (Continue on reverse if necessary and identify by block number)
FIELD	GROUP	SUB-GROUP	

19. ABSTRACT (Continue on reverse if necessary and identify by block number)

This paper reports density profiles and mean electrostatic potentials of a restricted primitive model double layer. Results for an asymmetric 2:1 salt, predicted by three different nonlocal free energy density functional approximations, are compared with Monte Carlo results and with those of Gouy-Chapman theory. Results for the diffuse layer potential are also compared with those of some recent theories of the double layer. The hard-sphere contribution to the free-energy functional is based on a nonlocal generic model functional proposed by Percus. We choose the Carnahan-Starling equation of state to calculate the free energy of the homogeneous hard-sphere mixture which enters in the hard-sphere functional. The mean spherical approximation for a neutral bulk electrolyte is used to model the electrostatic part of the non-uniform ion-ion correlations present in the interface. For singly charged counterions the agreement between the density functional approximations applied here and the Monte Carlo data is excellent. For doubly charged counterions the agreement is very good at high concentrations, but differs from
(continued)

20. DISTRIBUTION/AVAILABILITY OF ABSTRACT	21. ABSTRACT SECURITY CLASSIFICATION
☒ UNCLASSIFIED/UNLIMITED ☐ SAME AS RPT ☐ DTIC USERS	Unclassified
22a. NAME OF RESPONSIBLE INDIVIDUAL Henry S. White	22b. TELEPHONE (Include Area Code) (612) 625-6995 22c. OFFICE SYMBOL

DD FORM 1473, 84 MAR 83 APR edition may be used until exhausted. All other editions are obsolete.

SECURITY CLASSIFICATION OF THIS PAGE

TECHNICAL REPORT #10

(Abstract Continued)

the MC results in several aspects at low concentrations. The density functional theories are successful in predicting the extremum of the diffuse-layer potential as a function of surface charge present in the simulations.

NONLOCAL FREE ENERGY DENSITY FUNCTIONAL APPROXIMATIONS FOR THE ELECTRICAL DOUBLE LAYER; COMPARISON WITH MONTE CARLO RESULTS FOR 2:1 SALTS.

L. Mier-y-Teran*, Zixiang Tang, H. S. White, and H. T. Davis.

Department of Chemical Engineering and Materials Science,
University of Minnesota, Minneapolis, MN 55455

ABSTRACT

This paper reports density profiles and mean electrostatic potentials of a restricted primitive model double layer. Results for an asymmetric 2:1 salt, predicted by three different nonlocal free energy density functional approximations, are compared with Monte Carlo results and with those of Gouy-Chapman theory. Results for the diffuse layer potential are also compared with those of some recent theories of the double layer. The hard-sphere contribution to the free-energy functional is based on a nonlocal generic model functional proposed by Percus. We choose the Carnahan-Starling equation of state to calculate the free energy of the homogeneous hard-sphere mixture which enters in the hard-sphere functional. The mean spherical approximation for a neutral bulk electrolyte is used to model the electrostatic part of the non-uniform ion-ion correlations present in the interface. For singly charged counterions the agreement between the density functional approximations applied here and the Monte Carlo data is excellent. For doubly charged counterions the agreement is very good at high concentrations, but differs from the MC results in several aspects at low concentrations. The density functional theories are succesfull in predicting the extremum of the diffuse-layer potential as a function of surface charge present in the simulations.

* On sabbatical leave from Deparamento de Fisica, Universidad Autonoma Metropolitana-Iztapalapa, Apartado Postal 55-534, 09340 Mexico, D. F., Mexico.

I. INTRODUCTION

Recently, a nonlocal density functional theory for the electrical double layer was presented [1]. A double layer is the separation of charge which occurs in an electrolyte in the presence of an electrode. In these studies the restricted primitive model of an electrolyte (RPM) was used. In this very simplified model, the ions are modeled as charged hard spheres of equal diameter d and the solvent is represented as a uniform medium with dielectric constant .

In Ref.(1), the general formalism due to Mermin [2] is used to construct a grand potential functional for the interface. The hard-sphere contribution to the free energy functional is based on a nonlocal generic model functional proposed by Percus [3]. It was shown by Vanderlick et al. [4], that this generic functional can be used as a generating functional of several known nonlocal approaches. In particular, the generalized van der Walls (GVDW) model [5], the generalized hard-rod model (GHRM) [6,7] and the smoothed-density approximation (SDA) due to Tarazona [8] can be generated with this functional. This generic functional was extended to mixtures by Vanderlick et al. [9].

Using the GHRM, the density functional theory was applied in Ref.(1) to a planar interface for symmetric 1:1 and 2:2 RPM electrolytes. More recently [10], the same theory, combined with the GVDW model and the SDA was also applied to symmetrical 1:1 and 2:2 salts. In all cases, use was made of the analytic solution of the mean spherical approximation MSA [11] for the bulk electrolyte to approximate the electrostatic part of the nonuniform Ornstein-Zernike direct correlation function wich appears in the theory. In both works [1,10], the free energy of the hard-sphere system, which appears in the functional, was approximated with the Carnahan-Starling expression [12]. In Ref.(10), the Clausius equation of state was also used.

The results of Refs.(1,10) can be summarized as follows: the comparison of the density functional theory with the computer simulations of Torrie and Valleau [13,14] for symmetric electrolytes shows that, when combined with the Carnahan-Starling equation of state, the theory is very succesful in predicting density profiles and mean electrostatic potential functions for the RPM electrolyte. The theory correctly predicts the layering effects present in the computer simulations of 1:1 electrolytes at 1 M and high electrode charges [13], and the charge reversal phenomena which occurs in 2:2 electrolytes [14]. The three models studied are in very close agreement at low concentrations and low surface charge densities but the differences between them increases when charge or concentration are increased. The comparison with the MC data [13] for the diffuse layer potential as a function of the surface charge density [10] shows that the GHRM is superior to the other two models at high surface density charges for highly concentrated 1:1 electrolytes. This is probably due to a fortuitous cancelation of errors in the GHRM since the SDA, which is a better model for the non-uniform hard-sphere system [4], gives a better representation of the layering effects present at high density charges. The three models compared are only

in qualitative agreement with the MC data for the diffuse layer potential as a function of surface charge density for 2:2 salts [10].

In this article we report results of the density functional theory for 2:1 electrolytes for both positively and negatively charged electrodes. As in Ref.(10), we present a comparison between the GHRM, the GVDW model and the SDA. We also compare our results with those of the Gouy-Chapman [15,16] theory as modified by Stern [17] (MGC), and with those of some recent theories of the double layer. These include the most refined version of the modified Poisson-Boltzmann (MPB5) theory [18], the hypernetted chain/mean spherical approximation (HNC/MSA) theory [19] and the Born-Green-Yvon (YBG) with the closure introduced by Caccamo et al. [20].

As pointed out previously by several authors [14,19], results for 2:1 salts are interesting not only because their practical applications, but also because the MGC theory exhibit both qualitative agreement or disagreement, compared with the MC results, depending upon whether the counterion is monovalent or divalent.

This article is as follows. In Sec. II we briefly review the theory. We report our results in Sec. III and we conclude in Sec. IV with a disscusion.

II. THEORY

In Refs.(1) and (10) the formalism due to Mermin [2] was adopted to construct a model grand potential functional, $\Omega(\{\mathbf{n}\})$, for a mixture of charged particles in an external potential $v_\alpha(\mathbf{r})$. This functional of the density profiles can be written in the following form:

$$\begin{aligned}\beta\Omega(\{\mathbf{n}\}) = \beta\Omega(\{\mathbf{n}^i\}) + \beta\sum_\alpha \int d^3r\, n_\alpha(\mathbf{r}) v_\alpha(\mathbf{r}) \\ + \sum_\alpha \int d^3r\, n_\alpha(\mathbf{r})\, ln\left(n_\alpha(\mathbf{r})/n_\alpha^i\right) - \sum_\alpha \int d^3r\, \left[n_\alpha(\mathbf{r}) - n_\alpha^i\right] \\ + \sum_{\alpha\beta} \int\int d^3r\, d^3r'\, \left[n_\alpha(\mathbf{r}) - n_\alpha^i\right]\left[n_\beta(\mathbf{r}) - n_\beta^i\right] \int_0^1 d\lambda \int_0^\lambda d\lambda' c_{\alpha\beta}(\mathbf{r},\mathbf{r}';\lambda'),\end{aligned} \tag{2.1}$$

where $\beta = 1/kT$, T is the absolute temperature and k is Boltzmann's constant. In this equation $\Omega(\{\mathbf{n}^i\})$ is the grand free energy of a reference or initial state at the same temperature T, chemical potentials, μ_α, and volume V than the interface. The reference state was chosen to be absent of any external potential. It is a state of uniform density in which

$$n_\alpha^i(\mathbf{r}) = n_\alpha = \text{constant}. \tag{2.2}$$

In the obtention of Eq.(2.1), a lincar path was chosen for the functional integration. The path is characterized by a single parameter λ which varies from 0 to the unity. The function

$c_{\alpha\beta}(\mathbf{r},\mathbf{r}';\lambda)$ represents the Ornstein-Zernike direct correlation function of a nonuniform mixture at a particular point on the integration path.

The equilibrium density profiles, $n_\alpha(\mathbf{r})$, minimize the grand potential functional, $\Omega(\{\mathbf{n}\})$, for fixed $v_\alpha(\mathbf{r})$ and intermolecular potentials $u_{\alpha\beta}(\mathbf{r},\mathbf{r}')$. For a restricted primitive model electrolyte the pair potential can be separated into its Coulombic and short-range repulsive contributions

$$u_{\alpha\beta}(\mathbf{r},\mathbf{r}') = z_\alpha z_\beta e^2 u^c(|\mathbf{r}-\mathbf{r}'|) + u^r(|\mathbf{r}-\mathbf{r}'|), \tag{2.3}$$

where z_α is the valence of species α, e is the magnitude of the electronic charge,

$$u(r) = 1/\epsilon r, \tag{2.4}$$

and

$$\begin{aligned} u^r(r) &= \infty, \qquad r < d, \\ &= 0, \qquad r > d. \end{aligned} \tag{2.5}$$

It is also convenient to separate the Coulombic and short range contributions to the external potentials. The impenetrable wall produces a repulsive potential of the form,

$$\begin{aligned} v^r(x) &= \infty, \qquad x < d/2, \\ &= 0, \qquad x > d/2, \end{aligned} \tag{2.6}$$

where x is the shortest distance to the wall. The surface charge density, σ, gives rise to a one body Coulombic potential of the following form

$$v(x) = -2\pi\sigma|x|/\epsilon + C, \tag{2.7}$$

where C is a constant which determines the point of zero potential. By functional diferentiation of the grand potential functional w.r.t. $n(\mathbf{r})$, we obtain the following expression for the equilibrium density profiles:

$$\begin{aligned} ln(n_\alpha(\mathbf{r})/n_\alpha) = &-\beta\left(v_\alpha^r(\mathbf{r}) + ez_\alpha\psi(\mathbf{r})\right) \\ &+ \sum_\beta \int d^3r' \, [n_\beta(\mathbf{r}') - n_\beta] \int_0^1 d\lambda \Delta c_{\alpha\beta}(\mathbf{r},\mathbf{r}';\lambda) \\ &- \frac{\delta\Delta F^{HS}(\{\mathbf{n}\})}{\delta n_\alpha(\mathbf{r})}. \end{aligned} \tag{2.8}$$

In the last equation, $\psi(\mathbf{r})$ is the mean electrostatic potential, $\Delta c_{\alpha\beta}(\mathbf{r},\mathbf{r}')$ is the residual part of the direct correlation function defined by

$$c_{\alpha\beta}(\mathbf{r},\mathbf{r}') \equiv -\beta z_\alpha z_\beta e^2 u^c(|\mathbf{r}-\mathbf{r}'|) + c_{\alpha\beta}^{HS}(\mathbf{r},\mathbf{r}') + \Delta c_{\alpha\beta}(\mathbf{r},\mathbf{r}'), \tag{2.9}$$

and $c_{\alpha\beta}^{HS}(\mathbf{r},\mathbf{r}')$ is the hard sphere contribution to the function $c_{\alpha\beta}(\mathbf{r},\mathbf{r}')$. The last term on the right hand side of Eq.(2.8) is the functional derivative of the excess free energy change between the reference state and and the final state due to the hard sphere interaction [1]. The mean electrostatic potential is a solution of Poisson's equation. In the case of a planar interface, Poisson's equation can be integrated to give

$$\psi(x) = \frac{4\pi e}{\epsilon}\int_x^\infty dx'\,(x-x')\sum_\alpha z_\alpha n_\alpha(x'), \tag{2.10}$$

where the condition of overall electroneutrality,

$$e\int_0^\infty dx'\,\sum_\alpha z_\alpha n_\alpha(x') = -\sigma, \tag{2.11}$$

was imposed.

In order to obtain an expression for the hard-sphere excess free energy functional $\Delta F^{HS}(\{\mathbf{n}\})$, we make use of the generic functional proposed by Percus [3] as the three dimensional generalization of the Helmholtz free energy of an inhomogeneous hard rod system. This functional can be written for mixtures [9] as

$$F^{excess}(\{\mathbf{n}\}) = \sum_\alpha \int d^3r\,\bar{n}_\alpha^\nu(\mathbf{r}) F_0\left(\{\bar{\mathbf{n}}^\tau(\mathbf{r})\}\right), \tag{2.12}$$

where $\bar{n}_\alpha^\nu(\mathbf{r})$ and $\bar{n}_\alpha^\tau(\mathbf{r})$ are coarse grain densities which are defined as spatial averages of the local densities over certain small domains. For a mixture, the coarse grain densities are defined as

$$\bar{n}_\alpha^\nu(\mathbf{r}) = \int d^3r'\,\nu_\alpha(\mathbf{r}-\mathbf{r}';\{\mathbf{n}\})n_\alpha(\mathbf{r}'), \tag{2.13}$$

$$\bar{n}_\alpha^\tau(\mathbf{r}) = \int d^3r'\,\tau_\alpha(\mathbf{r}-\mathbf{r}';\{\mathbf{n}\})n_\alpha(\mathbf{r}'). \tag{2.14}$$

The weigthting functions $\nu_\alpha(\mathbf{r}-\mathbf{r}';\{\mathbf{n}\})$ and $\tau_\alpha(\mathbf{r}-\mathbf{r}';\{\mathbf{n}\})$, which in the most general case are functionals of the density distributions must be normalized, i.e.,

$$\int d^3r'\,\nu_\alpha(\mathbf{r}-\mathbf{r}';\{\mathbf{n}\}) = \int d^3r'\,\tau_\alpha(\mathbf{r}-\mathbf{r}';\{\mathbf{n}\}) = 1. \tag{2.15}$$

By changing the specific form of weighting functions in Eqs.(2.13) and (2.14) different model density functionals can be generated [4]. In this work we solved Eq.(2.8) for the three model functionals mentioned before; the GVDW, the GHRM, and the SDA due to Tarazona. Here we briefly summarize the specific forms of the weigthting functions $\nu_\alpha(\mathbf{r}-\mathbf{r}';\{\mathbf{n}\})$ and $\tau_\alpha(\mathbf{r}-\mathbf{r}';\{\mathbf{n}\})$ for these three models. For the GVDW model, we have

$$\nu_\alpha(\mathbf{r}-\mathbf{r}';\{\mathbf{n}\}) = \delta(\mathbf{r}-\mathbf{r}'), \tag{2.16}$$

$$\tau_\alpha(\mathbf{r}-\mathbf{r}';\{\mathbf{n}\}) = H(d-|\mathbf{r}-\mathbf{r}'|)/(4\pi d^3/3), \tag{2.17}$$

where $\delta(\mathbf{r})$ the Dirac delta function and $H(r)$ is the Heaviside step function defined by

$$\begin{aligned} H(r) &= 1, \qquad r > 0, \\ &= 0, \qquad r < 0. \end{aligned} \tag{2.18}$$

For the GHRM [6,7],

$$\nu_\alpha(\mathbf{r}-\mathbf{r}';\{\mathbf{n}\}) = \delta(d/2-|\mathbf{r}-\mathbf{r}'|)/(4\pi(d/2)^2), \tag{2.19}$$

$$\tau_\alpha(\mathbf{r}-\mathbf{r}';\{\mathbf{n}\}) = H(d/2-|\mathbf{r}-\mathbf{r}'|)/(4\pi(d/2)^3/3), \tag{2.20}$$

whereas for the SDA [8], we have

$$\nu_\alpha(\mathbf{r}-\mathbf{r}';\{\mathbf{n}\}) = \delta(\mathbf{r}-\mathbf{r}'), \tag{2.21}$$

$$\begin{aligned} \tau_\alpha(\mathbf{r}-\mathbf{r}';\{\mathbf{n}\}) = w_\alpha^{(0)}(|\mathbf{r}-\mathbf{r}'|) &+ \sum_\beta w_{\alpha\beta}^{(1)}(|\mathbf{r}-\mathbf{r}'|)\bar{n}_\beta^\tau(\mathbf{r}) \\ &+ \sum_{\beta\gamma} w_{\alpha\beta\gamma}^{(2)}(|\mathbf{r}-\mathbf{r}'|)\bar{n}_\beta^\tau(\mathbf{r})\bar{n}_\gamma^\tau(\mathbf{r}). \end{aligned} \tag{2.22}$$

In the case of a restricted primitive model electrolyte, all the ions have the same diameter. As a result of this simplification, the w's become to be independent on the species, and we can rewrite Eq.(2.22) as

$$\begin{aligned} \tau_\alpha(\mathbf{r}-\mathbf{r}';\{\mathbf{n}\}) = w^{(0)}(|\mathbf{r}-\mathbf{r}'|) &+ w^{(1)}(|\mathbf{r}-\mathbf{r}'|)\sum_\beta \bar{n}_\beta^\tau(\mathbf{r}) \\ &+ w^{(2)}(|\mathbf{r}-\mathbf{r}'|)(\sum_\beta \bar{n}_\beta^\tau(\mathbf{r}))^2, \end{aligned} \tag{2.23}$$

Thus, in the SDA, the density dependent weighting functions $\tau_\alpha(\mathbf{r}-\mathbf{r}';\{\mathbf{n}\})$ are expressed as a truncated series in the nonlocal densities $\bar{n}_\beta^\tau(\mathbf{r})$. The coefficients $w^{(0)}(|\mathbf{r}-\mathbf{r}'|)$, $w^{(1)}(|\mathbf{r}-\mathbf{r}'|)$ and $w^{(2)}(|\mathbf{r}-\mathbf{r}'|)$ are density independent weighting functions which satisfy the following properties:

$$\int d^3r\, w^{(i)}(|\mathbf{r}|) = \delta_{0i}, \qquad i = 0,1,2. \tag{2.24}$$

With $\tau_\alpha(\mathbf{r}-\mathbf{r}';\{\mathbf{n}\})$ defined in this way, and using Eq.(2.14), $\bar{n}_\alpha^\tau(\mathbf{r})$ can now be expressed as

$$\bar{n}_\alpha^\tau(\mathbf{r}) = \bar{n}_\alpha^{(0)}(\mathbf{r}) + \bar{n}_\alpha^{(1)}(\mathbf{r})\sum_\beta \bar{n}_\beta^\tau(\mathbf{r}) + \bar{n}_\alpha^{(2)}(\mathbf{r})(\sum_\beta \bar{n}_\beta^\tau(\mathbf{r}))^2, \tag{2.25}$$

where

$$\bar{n}_\alpha^{(i)}(\mathbf{r}) = \int d^3r' w^{(i)}(|\mathbf{r}-\mathbf{r}'|)n_\alpha(\mathbf{r}'), \qquad i = 0,1,2. \tag{2.26}$$

In the SDA the coefficients w are determined by requiring the direct correlation function $c^{HS}(|\mathbf{r}-\mathbf{r}'|)$ of a uniform hard-sphere fluid obtained from the second order functional derivative of the excess free-energy functional, F^{excess}, be close to that of the Percus-Yevick approximation for the hard-sphere uniform fluid to the second order in density [8]. The prescription for the density independent weighting functions is

$$\begin{aligned} w^{(0)}(r) &= \frac{3}{4\pi d^3}, && r < d, \\ &= 0, && r > d, \end{aligned} \tag{2.27a}$$

$$\begin{aligned} w^{(1)}(r) &= 0.475 - 0.648\left(\frac{r}{d}\right) + 0.113\left(\frac{r}{d}\right)^2, && r < d, \\ &= 0.288\left(\frac{d}{r}\right) - 0.924 + 0.764\left(\frac{r}{d}\right) - 0.187\left(\frac{r}{d}\right)^2, && d < r < 2d, \\ &= 0, && r > 2d, \end{aligned} \tag{2.27b}$$

$$\begin{aligned} w^{(2)}(r) &= \frac{5\pi d^3}{144}\left[6 - 12\left(\frac{r}{d}\right) + 5\left(\frac{r}{d}\right)^2\right], && r < d, \\ &= 0, && r > d. \end{aligned} \tag{2.27c}$$

In the SDA, the total coarse-grained density, $\sum_\alpha \bar{n}_\alpha^r$, required in our computations is given by the following root of the quadratic equation, Eq.(2.25),

$$\sum_\alpha \bar{n}_\alpha^r(\mathbf{r}) = \frac{1 - \sum_\alpha \bar{n}_\alpha^{(1)}(\mathbf{r}) - \left[\left(1 - \sum_\alpha \bar{n}_\alpha^{(1)}(\mathbf{r})\right)^2 - 4\left(\sum_\alpha \bar{n}_\alpha^{(0)}(\mathbf{r})\right)\left(\sum_\alpha \bar{n}_\alpha^{(2)}(\mathbf{r})\right)\right]^{\frac{1}{2}}}{2\bar{n}^{(2)}(\mathbf{r})}. \tag{2.28}$$

According to Eq.(2.8), our description of the electrical interface is not complete without the kwoledge of the inhomogeneous residual correlation function $\Delta c_{\alpha\beta}(\mathbf{r},\mathbf{r}';\lambda)$ and the excess free energy per particle F_0 of a homogeneous hard-sphere fluid. We approximate the function $\Delta c_{\alpha\beta}(\mathbf{r},\mathbf{r}';\lambda)$ with the function $\Delta c_{\alpha\beta}(|\mathbf{r}-\mathbf{r}'|)$ of a neutral bulk electrolyte and use the MSA expression for this function given by [11]

$$\begin{aligned} \Delta c_{\alpha\beta}(r) &= -\beta\frac{q_\alpha q_\beta}{\epsilon}\left[2\left(\frac{B}{d}\right) - \left(\frac{B}{d}\right)^2 r - \frac{1}{r}\right], && r < d, \\ &= 0, && r > d, \end{aligned} \tag{2.29}$$

where

$$B = \frac{1}{\kappa_D^*}\left[\kappa_D^* + 1 - (1 + 2\kappa_D^*)^{\frac{1}{2}}\right],$$

and $\kappa_D^* = \kappa_D d$. The quantity κ_D is the inverse Debye screening length given by

$$\kappa_D^2 = (4\pi\beta e^2/\epsilon)\sum_\alpha n_\alpha z_\alpha^2. \tag{2.30}$$

In this work we use the quasiexact Carnahan-Starling formula for the excess free energy per particle of a homogeneous hard-sphere fluid [12]. For the RPM electrolyte we can use the expression

$$\beta F_0(n) = \frac{\eta(4-3\eta)}{(1-eta)^2}, \qquad \eta = \pi n d^3/6, \tag{2.31}$$

for the one component hard-sphere fluid.

III. RESULTS

In this work we have carried out calculations for 2:1 electrolytes at bulk concentrations of 0.005, 0.05 and 0.5 M. For the two latter concentrations we considered both positive and negative surface charge densities σ. For concentration of 0.005 M the MC data reported [14] are for negative values of σ only. Since we are interested in a comparison of our results with the data obtained via computer simulation, we restricted our calculations at bulk concentration of 0.005 M to negative values of σ. For positive surface charge, the counterions are singly charged ions , while for negative surface charge the counterions are doubly charged.

In order to solve Eq.(2.6) we employed the finite-element numerical techniques described elsewhere [21]. As in Refs.(1) and (10), we used quadratic Lagrange interpolating polynomials as basis functions for solving Eq.(2.6) for the GHRM and linear or "chapeau" functions for solving the same equation for the GVDW model and the SDA. We generated solutions in the domain $d/2 \leq x \leq R$, where x is the distance to the wall and R is the cutoff distance used as the upper limit in the integrals. A uniform mesh of N points was used in all the cases. Both N and R are strongly dependent on the concentration of the bulk electrolyte.

A Newton iterative scheme was used to solve the set of non-linear algebraic equations for the values of the reduced density profiles at the positions of the nodes: $g_{\alpha i} = n_\alpha(x_i)/n_\alpha$. The iterative process is continued until the Euclidean norm of the updates after the iteration k+1 becomes less than 10^{-10}, i.e.,

$$\left[\frac{\sum_\alpha \sum_i \left(g_{\alpha i}^{(k+1)} - g_{\alpha i}^{(k)}\right)^2}{2N}\right]^{\frac{1}{2}} < 10^{-10}. \tag{3.1}$$

As a second internal test of our calculations we also have cheked the agreement of the electroneutrality condition, Eq.(2.11). This equation was satisfied to at least five significant figures in all our calculations.

We found convenient to use dimensionless parameters. The dimensionless surface charge density is $\sigma^* = \sigma d^2/e$. The dimensionless mean electrostatic potential is $\psi^*(x) =$

$\beta e\psi(x)$. The distance x is reduced by the diameter d. As in our previous work, in order to compare with the MC data of Valleau and co-workers [14], we fixed the plasma parameter to $\Gamma^* = \beta e^2/\epsilon d = 1.6809$. This value of Γ^* corresponds to T=298 K, $\epsilon = 78.5$ and d= 4.25Å.

Our results for the diffuse layer potential at several values of the surface charge, σ^* , for 2:1 electrolytes are summarized in Table I. For comparison, in the same table we also display the MC results of Torrie and Valleau [14], the results of the MGC theory [15-17], the BGY theory of Caccamo et al. [20], those corresponding to the MPB5 theory [18], and HNC/MSA results due to Lozada-Cassou and Henderson [19]. For positive values of σ^*, the agreement between the results of the density functional theories presented in this article and the MC data is excellent. The GHRM theory is slightly superior to the other two density functional theories for positive σ^* . For negative surface charges, the agreement between our results and the MC data is only fair at low concentrations but considerable improves at the higher concentration of 0.5 M. The GVDW theory and the SDA are slightly better than the GHRM for the negative values of σ^* investigated in this work.

A comparison of the results of the three density functional theories with the MGC theory and MC data is presented in Fig. 1. This figure shows the dimensionless diffuse layer potential, $\psi^*(0) = \beta e\psi(0)$ as a function of the electrode charge density σ^* for c = 0.005, 0.05 and 0.5 M. The MGC theory, which neglects the effects due to the finite size of the ions, overestimates the thickness of the double layer and predicts a monotonic rise for the diffuse layer potential as a function of σ^*. As has been pointed out by other authors [14], for positive surface charge, the behavior of the diffuse layer potential as a function of σ^* is very reminiscent of that of 1:1 electrolytes. For negative surface charges, the monotonic behavior of the MGC theory is in significant disagreement with the MC data, since the simulation results present a minimum in the diffuse layer potential as a function of σ^*. The density functional theories predict the presence of that minimun. Since the results of the GVDW theory are undistinguishable from those of the SDA with the scales used in all our plots, in what follows we only show one line for these two approximations. For c = 0.005 M, the results of the three density functional theories are undistinguishable on the plot.

We proceed now to examine the information contained in the ionic density profiles and mean electrostatic potential profiles. For positive surface densities and low concentrations, the behavior of the double layer is very similar to that found in 1:1 systems. Thus we describe the behavior at higher concentrations where more interesting phenomenae are present. In Fig. 2 we display the density profiles at 0.5 M and σ^* =0.20. The solid lines correspond to the GHRM theory, while the dot-dashed lines correspond to the GVDW theory and SDA. The circles correspond to the MC data of Torrie and Valleau [14]. The dashed lines are the MGC density profiles calculated with the analytic solution for 2:1 RPM electrolytes found by Grahame [22]. As shown in Fig. 2, the three density functional theories predict a counterion profile with a very shallow minimum around $x = 2.5d$. To this minimum, corresponds a maximum in the coion density profile. Note that the position

of the plate has been shifted to $x = -d/2$ in all our plots. The MC results seem to present the same oscillatory behavior, but it is partially hiden by the statistical noise. As usual, the classical MGC theory predicts monotonic density profiles. The oscillatory behavior is also apparent in the mean electrostatic potential as a function of the distance to the wall. In Fig. 3 we can see how the MC data for the function $\psi(x)$ have a change in sign around $x = 1.5d$ and present a shallow minimun. The three density functional theories studied predict quite well the location and size of this minimum in $\psi(x)$.

We now shift our attention towards systems with negative surface charges. This situation corresponds to a system with doubly charged counterions and singly charged coions. For systems with low surface density, the behavior of the density profiles and potential profile is monotonic. This is the case for $c = 0.005$ M and $\sigma^* =$ -0.05, see Fig. 4, where the results of the three density functional theories for the function $\psi(x)$ are coincident up to the scale presented. Even when the results obtained with the density functional theories are in considerable improvement over the MGC theory, appreciably overestimate the interfacial thickness.

At higher concentration and higher surface charges the MC profiles are no longer monotonic. In Fig. 5 we present MC density profiles at $c = 0.05$ M and $\sigma^* = -0.20$. The coion density profile obtained in the MC simulation [14] has a peak around $x = 1.5d$. In the same figure we display the profiles obtained with the density functional theories studied in this paper and those of the MGC theory The profiles predicted by the density functional theories are still monotonic but show a clear tendency towards an oscillatory behavior. As before, the differences between the GVDW and the SDA are negligible. Differences between the GHRM theory and the other two density functional theories are also very small in this case. The three theories produce coion density profiles which are undistinguishable in the figure. At the larger surface charge of $\sigma^* = -0.284$ and the same concentration $c = 0.05$ M, the MC data show a very small charge inversion in between $x = 2.5d$ and $4.5d$; see Fig. 6. The profiles predicted by the density functional theories are still monotonic and the differences between them continue to be very small. Of course, the MGC theory profiles are monotonic. The charge inversion phenomenae present in the MC data at these conditions, produces an oscillatory behavior in the mean electrostatic potential profile; see Fig. 7.

The oscillatory behavior in the MC data is more evident at higher concentrations. In Fig. 8 we present a comparison of the MC density profiles with those obtained with the density functional theories studied here at $c = 0.5$ M and $\sigma^* = -0.1704$. The charge reversal phenomenae is very pronounced at these conditions. For comparison, in the same figure we display the results of the MGC theory. The agreement between the density functional theories and the simulation results is good here. Again, the differences between the three density functional theories are very small. The charge reversal found at $c = 0.5$ M and $\sigma^* = -0.1704$ produces a relatively deep minimum in the mean electrostatic potential profile. In Fig. 9 we compare the results of the density functional theories for the function $\psi(x)$ with the MC results. The agreement between the theories theories studied here and the simulation results is good, but the theories clearly underestimate the deepness of the minimum.

IV. SUMMARY

In this article we applied three different nonlocal free energy density functional approximations to the problem of a double layer consisting of a 2:1 RPM electrolyte solution in the presence of a planar electrode. Previously, we applied these theories to a double layer in equilibrium with symmetrical 1:1 and 2:2 salts [1,10]. These nonlocal density functional approximations are based on the generic functional proposed by Percus [3] and generalized to mixtures by Vandelick et al. [9]. This functional attempts to account for the nonlocal effects due to the finite size of fluid particles by incorporating coarse-grain densities. The approximations studied here provide three different models of weighting functions for the specification of the coarse-grain densities. Following Refs.(1) and (10), we use the Carnahan-Starling [12] equation of state to approximate the free energy of a homogeneous hard-sphere mixture. This latter quantity is required as an imput by the functional. The residual electrostatic part of the inhomogeneous direct correlation functions are approximated with those of the neutral bulk electrolyte which is in equilibrium with the interface. We use the analytical solution of the MSA for bulk electrolytes [11] for the latter.

The density functional approximations compared in this article, are quantitatively correct in their predictions of density profiles and mean electrostatic potential functions of 2:1 electrolytes when the counterions are singly charged. The values of the diffuse layer potential obtained with these theories for positive σ, are in excellent agreement with the MC data within the intervals of composition and surface charge explored. The GHRM is slightly better than the other theories studied in this work for singly charged counterions. This result is reminiscent of that found for 1:1 electrolytes [10]. At very high charges, one would expect the appearence of the layering phenomenon observed in 1:1 salts. The differences between the theories compared and the simulation results, grow very slowly when σ is increased.

The theories compared in this article correctly predict the qualitative asymmetry with respect to the sign of the surface charge found in the MC data of the diffuse layer potential. However, only at high concentration the theories give a satisfactory quantitative prediction of this property when the counterions are doubly charged. At low concentrations and small negative surface charges, the theories correctly predict the monotonic behavior of the density and mean electrostatic potential profiles, but fail to predict the oscillatory behavior present in the MC results when the surface charge is increased. At high concentration the density and mean electrostatic potential profiles obtained in this work show the charge reversal effect in agreement with the MC simulations.

For singly charged counterions, the theories studied here compete in accuracy with the results obtained by Plischke and Henderson [23] by solving the inhomogeneous Ornstein-Zernike (OZ) equation for the pair correlation function together with the Lovett-Mou-Buff-Wertheim equation and the hypernetted chain closure. For doubly charged counterions.

the OZ/LMBW theory shows to be superior by predicting the oscillatory behavior present in the density profiles and mean electrostatic potential at low concentrations and high surface charges.

The GVDW model is the zero order approximation of the SDA. Thus, the very small differences found between the predictions of these two theories within the intervals of composition and σ studied, for both positive and negative values of σ, show that the zero order term in the weighting functions of the SDA is extremely dominant over the other two terms in this regime.

ACKNOWLEDGMENTS

LMyT gratefully acknowledges the hospitality extended to him by the Minnesota Supercomputer Institute and the partial support given to him by CONACYT, Mexico. The Office Naval Research, the National Science Foundation, and the Minnesota Supercomputer Institute provided support for this work.

REFERENCES

1. L. Mier y Terán, S. H. Suh, H. S. White, and H. T. Davis. Submitted to Journal of Chemical Physics (1989).
2. N. D. Mermin, Phys. Rev. A 137, 1441 (1965).
3. J. K. Percus, J. Chem. Phys. 75, 1316 (1981).
4. T. K. Vanderlick, L. E. Scriven, and H. T. Davis, J. Chem. Phys. 90, 2422 (1989).
5. S. Nordholm, M. Johnson, and B. C. Freasier, Aust. J. Chem. 33, 2139 (1980); M. Johnson and S. Nordholm, J. Chem. Phys. 75, 1953 (1981).
6. A. Robledo and C. Varea, J. Stat. Phys. 26, 513 (1981).
7. J. Fischer and U. Heinbuch, J. Chem. Phys. 88, 1909 (1988).
8. P. Tarazona, Phys. Rev. A 31, 2672 (1985); P. Tarazona, U. Marini Bettolo Marconi, and R. Evans, Mol. Phys. 60, 573 (1987).
9. T. K. Vanderlick, H. T. Davis, and J. K. Percus, to appear in J. Chem. Phys. (1989).
10. Z. Tang, L. Mier y Teran, H. S. White, and H. T. Davis. In preparation.
11. E. Waismann and J. L. Lebowitz, J. Chem. Phys. 56, 3086 (1972); 56, 3093 (1972).
12. N. F. Carnahan and K. E. Starling, J. Chem. Phys. 51, 635 (1969); 53, 600 (1970).
13. G. M. Torrie and J. P. Valleau, J. Chem. Phys. 73, 5087 (1980); G. M. Torrie, J. P. Valleau, and G. N. Patey, ibid. 76, 4615 (1982); J. P. Valleau and G. M. Torrie, ibid. 76, 4623 (1982).
14. G. M. Torrie and J. P. Valleau, J. Phys. Chem. 86, 3251 (1982).
15. G. Gouy, J. Phys. 9, 451 (1910).
16. D. L. Chapman, Philos. Mag. 25, 475 (1913).
17. O. Stern, Z. Electrochem. 30, 508 (1924).
18. C. W. Outhwaite and L. Bhuiyan, J. Chem. Soc. Faraday Trans. 2 79, 707 (1983).
19. M. Lozada-Cassou and D. Henderson, J. Phys. Chem. 87, 2821 (1983).
20. C. Caccamo, G. Pizzimenti, and L. Blum, J. Chem. Phys. 84, 2327 (1986).
21. L. Mier y Teran, A. H. Falls, L. E. Scriven, and H. T. Davis, Proceeding 8th Symposium of Thermophysical Properties, ed. J. V. Sengers, American Society of Mechanical Engineers, New York,(1982). Vol. 1, pp. 45-56; L. Mier y Teran, E. Diaz-Herrera, M. Lozada-Cassou, and D. Henderson, J. Phys. Chem. 92, 6408 (1988); L. Mier y Teran, E. Diaz-Herrera, M. Lozada- Cassou, and R. Saavedra-Barrera, J. Comput. Phys. 84, 326 (1989).
22. D. C. Grahame, J. Chem. Phys. 21, 1054 (1953).
23. M. Plischke and D. Henderson, J. Chem. Phys. 88, 2712 (1988); 90, 5738 (1989).

TABLE I. Diffuse layer potential for 2:1 electrolytes.

	MC	MGC	BGY	MPB5	HNC/MSA	GHRM	GvdW	SDA
			0.005 M					
-0.01	-0.91(0.02)	-0.959	--	--	--	-0.947	-0.947	-0.947
-0.02	-1.37(0.01)	-1.518	--	--	--	-1.485	-1.484	-1.484
-0.05	-1.87(0.03)	-2.381	--	--	--	-2.233	-2.228	-2.228
			0.05 M					
-0.05	-1.05(0.01)	-1.315	-1.11	-1.05	-1.158	-1.160	-1.156	-1.156
-0.0975	-1.21(0.06)	-1.916	-1.476	-1.21	-1.511	-1.522	-1.505	-1.505
-0.126	-1.26(0.03)	-2.161	-1.597	-1.27	-1.577	-1.596	-1.568	-1.569
-0.20	-1.18(0.03)	-2.612	-1.739	-1.27	-1.497	-1.551	-1.481	-1.485
-0.284	-1.02(0.03)	-2.959	-1.74	-1.27	-1.176	-1.288	-1.153	-1.164
0.04294	1.73(0.02)	1.740	1.705	1.70	1.89	1.675	1.672	1.672
0.18	3.99(0.05)	4.324	4.04	--	3.89	4.005	3.922	3.922
			0.5 M					
-0.05	-0.40(0.02)	-0.547	-0.372	-0.373	-0.311	-0.317	-0.311	-0.312
-0.099	-0.50(0.01)	-0.951	-0.509	-0.463	-0.462	-0.476	-0.462	-0.463
-0.1704	-0.46(0.01)	-1.379	-0.574	-0.460	-0.482	-0.518	-0.480	-0.484
-0.24	-0.35(0.03)	-1.683	-0.557	-0.411	-0.351	-0.425	-0.351	-0.360
0.0989	1.04(0.02)	1.308	0.97	0.986	0.966	0.988	0.965	0.967
0.20	1.94(0.03)	2.364	1.875	1.85	1.806	1.914	1.814	1.831

a) G. M. Torrie and J. P. Valleau, Ref.(14). Statistical uncertainty is shown in parentheses.
b) C. Caccamo, G. Pizzimenti, and L. Blum, Ref.(20).
c) C. W. Outhwaite and L. B. Bhuiyan, Ref.(18).
d) M. Lozada-Cassou and D. Henderson. Published in Ref.(20).

FIGURE CAPTIONS

Fig. 1 Reduced diffuse layer potential, $\beta e\psi(0)$, as a function of the charge density, $\sigma d^2/e$, for 2:1 electrolytes. Solid lines represent the results of the GHRM, dot dashed lines the results of GVDW and SDA. The results displayed are for 0.005, 0.05 and 0.5 M. Solid squares, open circles, and solid circles are the corresponding MC results. Dashed lines are the results of the MGC theory.

Fig. 2 Reduced density profiles $n(x)/n$ for a 2:1 electrolyte at $c = 0.5$ M and $\sigma^* = 0.2$. The dots are the MC results. The dashed lines correspond to the MGC theory, the solid lines to the GHRM, and the dot dashed lines to the GVDW and SDA. Note that the wall is at $x = -d/2$.

Fig. 3 Reduced mean electrostatic potential profile at $c = 0.5$ M and $\sigma^* = 0.2$ Symbols as in Fig.2.

Fig. 4 Reduced mean electrostatic potential profile for a 2:1 RPM electrolyte at $c = 0.005$ M and $\sigma^* = -0.05$. The dots are the MC results of Ref.(13), The dashed line correspond to the MGC theory, and the solid line to the density functional approximations used in this work. At the low concentration and surface charge corresponding to this figure, the results of the three density functional approximations are undistinguishable on the plot.

Fig. 5 Reduced density profiles, $n(x)/n$, for a 2:1 electrolyte at $c = 0.05$ M and $\sigma^* = -0.2$. The dots are the MC results. The solid lines correspond to the GHRM, and the dot dashed lines to the GVDW and SDA. Dashed lines are the results of the MGC theory.

Fig. 6 Reduced density profiles, $n(x)/n$, for a 2:1 electrolyte at $c = 0.05$ M and $\sigma^* = -0.284$. All symbols as in Fig. 5.

Fig. 7 Reduced mean electrostatic potential profile for a 2:1 electrolyte at $c = 0.05$ M and $\sigma^* = -0.284$. All symbols as in Fig. 5.

Fig. 8 Reduced density profiles, n(x)/n, for a 2:1 electrolyte at $c = 0.5$ M and $\sigma^* = -0.1704$. The dots are the MC results. The solid lines correspond to the GHRM, and the dot dashed lines to the GVDW and SDA. Dashed lines are the results of the MGC theory. The density functional theories predict the charge reversal phenomenon.

Fig. 9 Reduced mean electrostatic potential profile for a 2:1 electrolyte at $c = 0.5$ M and $\sigma^* = -0.1704$. The dots are the MC results. The solid line correspond to the GHRM, and the dot dashed line to the GVDW and SDA. The dashed line corresponds to the MGC theory.

2:1
GHRM —
MGC - - -
T + G v dW —·—

fig. 1

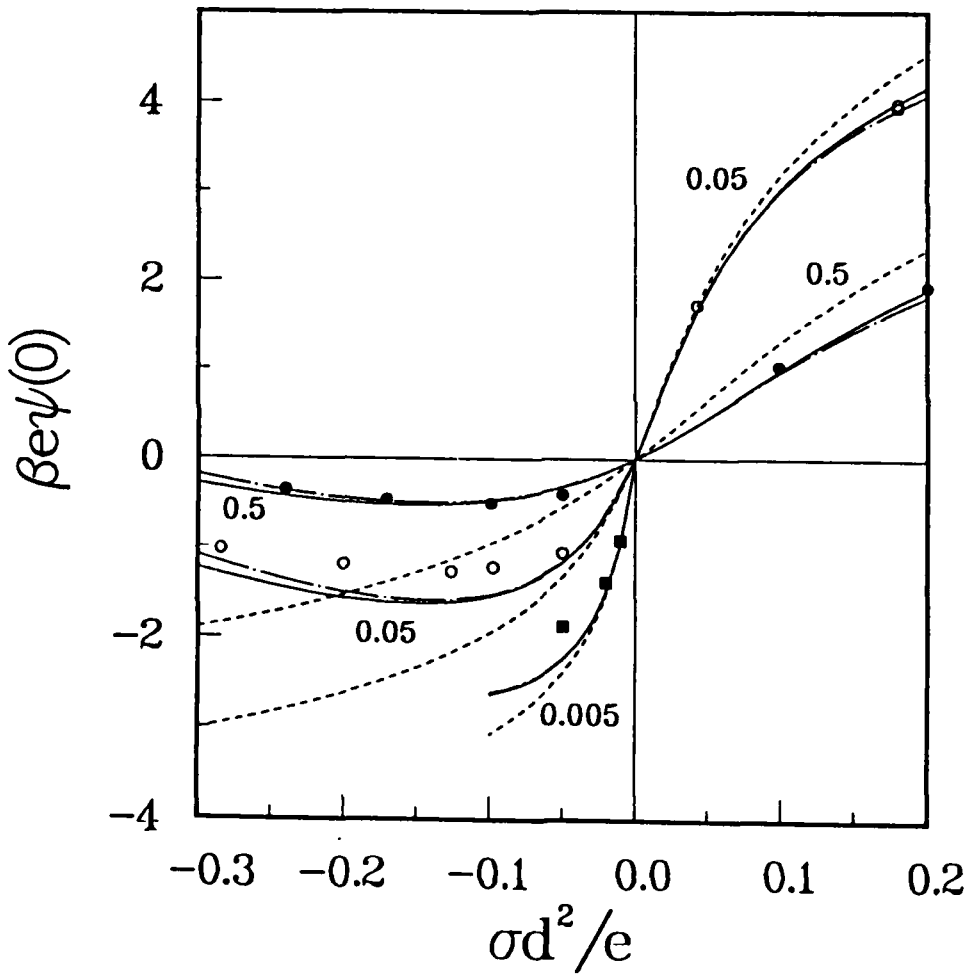

2:1

0.5 M

$\Gamma^* = 0.20$

GHRM ——

MGC - - -

T+GvdW —·—

Fig. 2

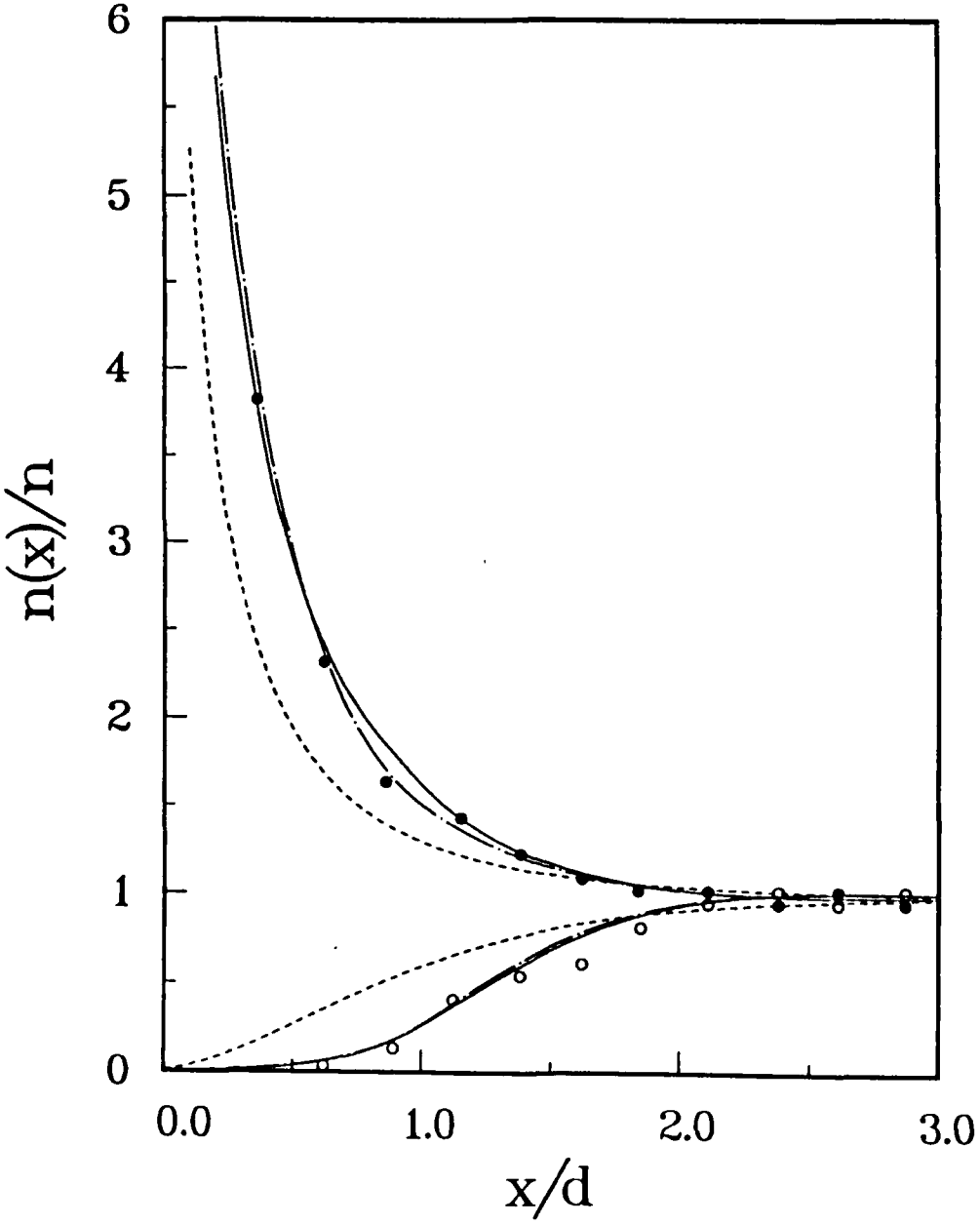

2:1

C = 0.5 M

$\Gamma^* = 0.20$

GHRM ——

MGC - - - -

T+GvdW —·—

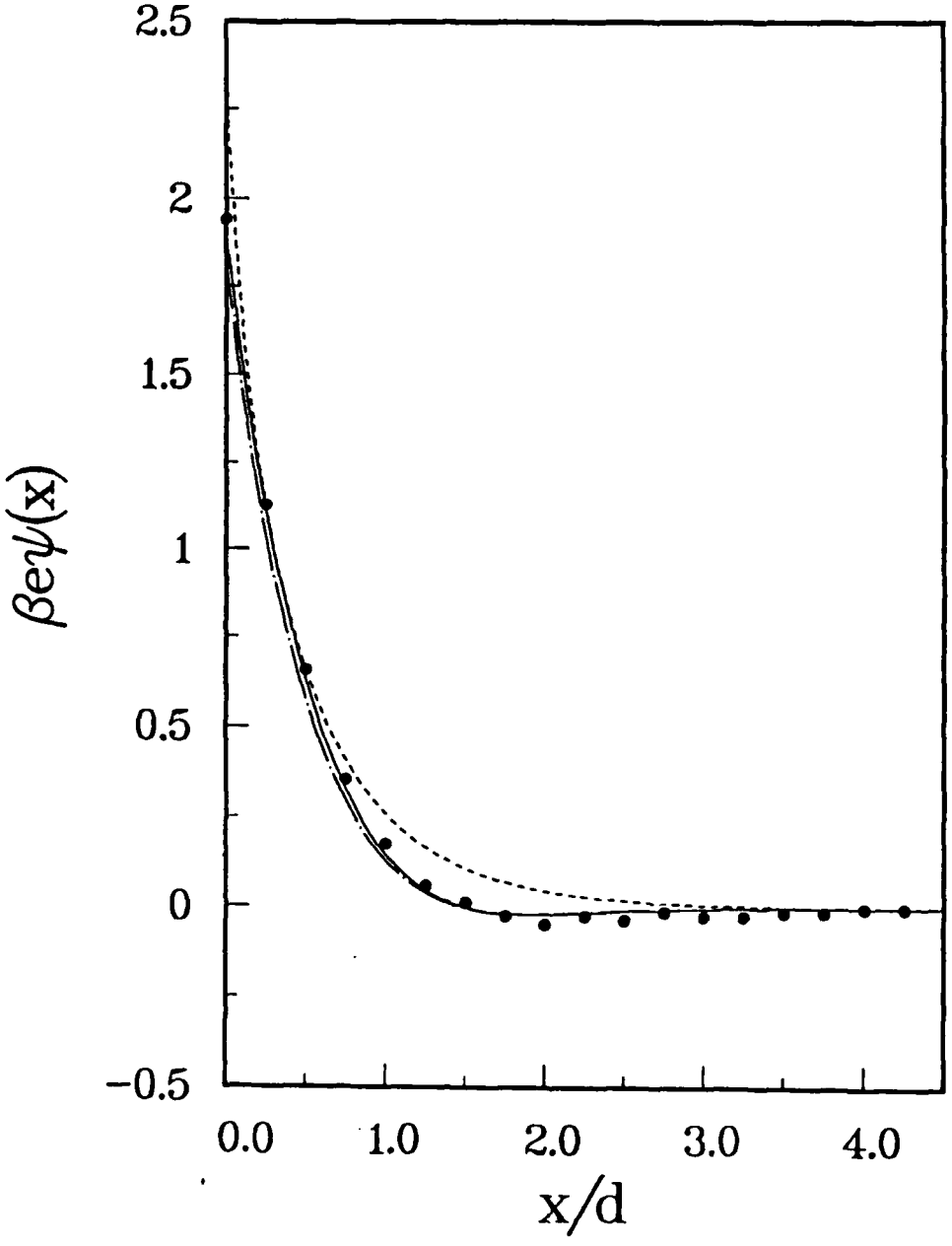

Fig. 3

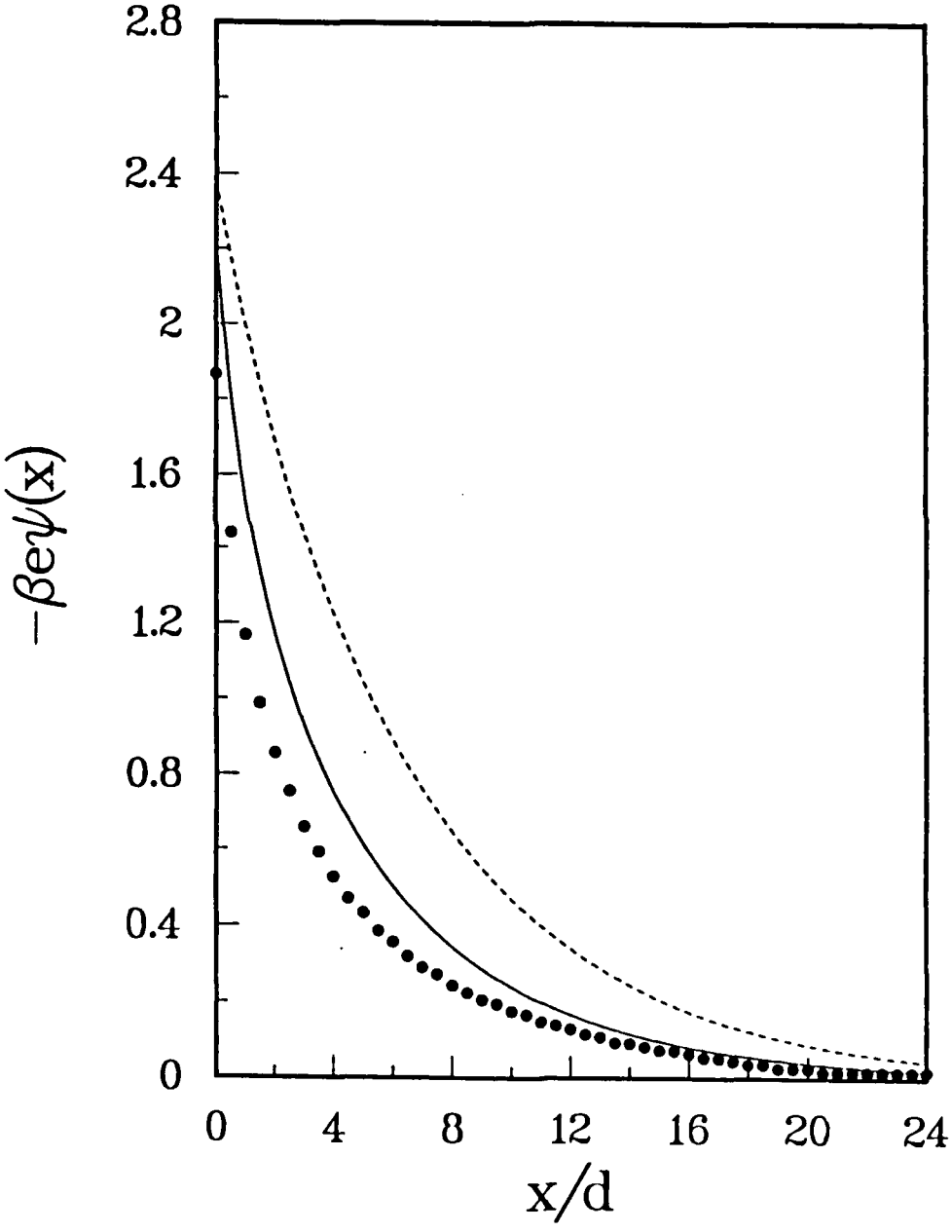

2:1

0.005 M

$\sigma^* = -0.05$

GHRM
T
GvdW } ——

• MC

---- MGC

Fig. 4

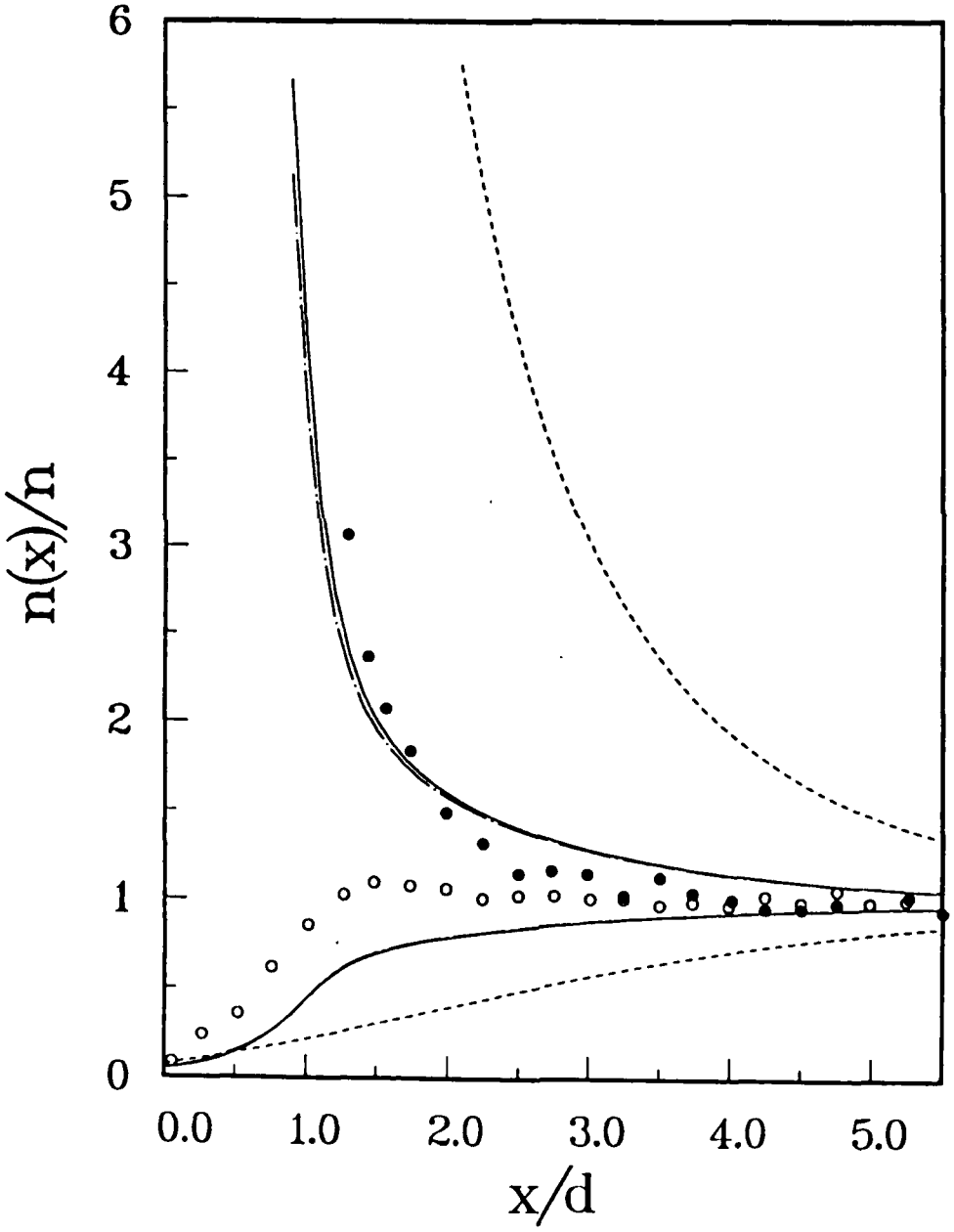

2:1

0.05 M

$\sigma^* = -0.20$

GHRM ——

MGC - - - -

T —·—

Fig. 5

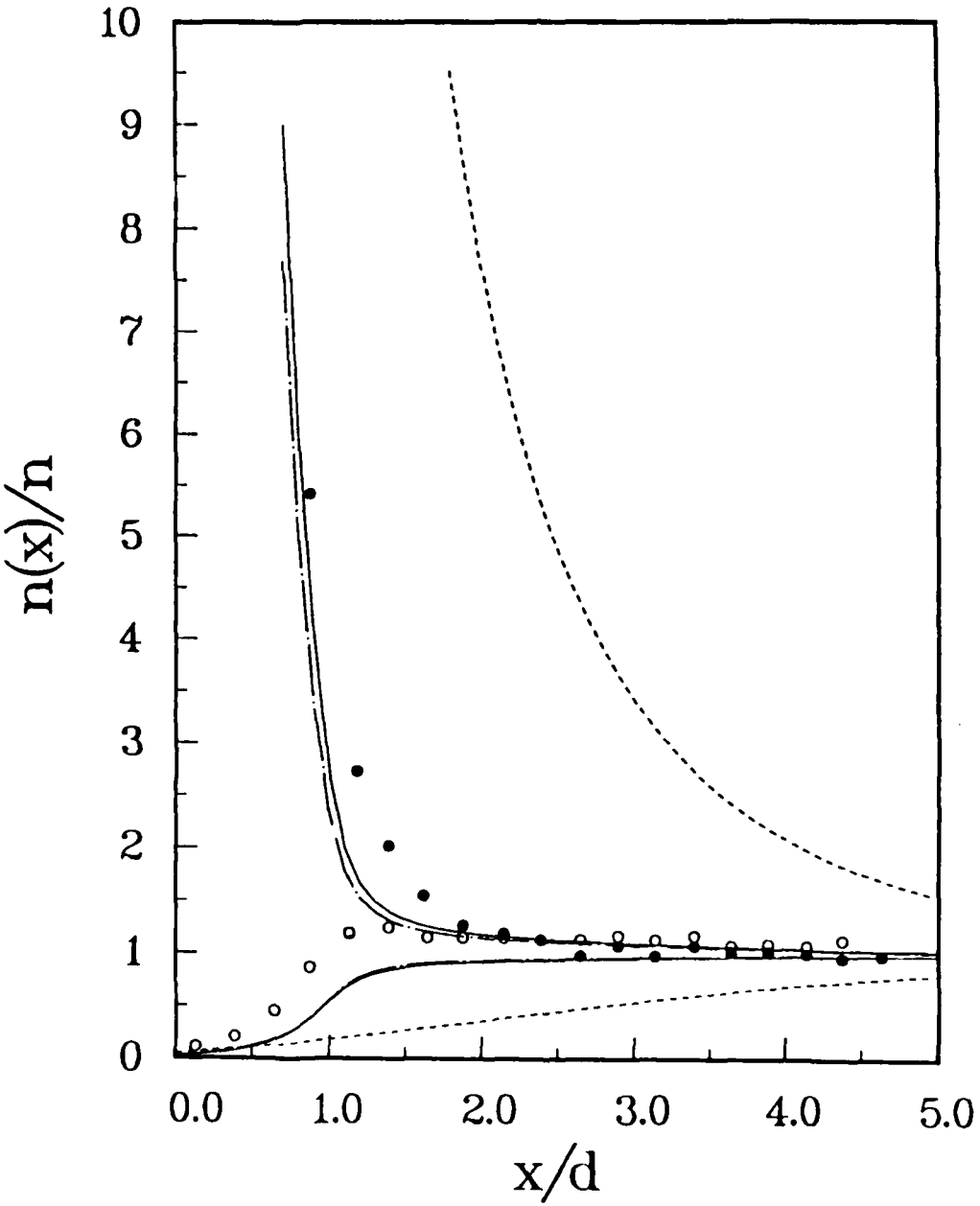

2:1
0.05 M
$\sigma = -0.284$

GHRM ——
MGC - - - -
T + GvdW —·—
MC ●, ○

Fig. 6

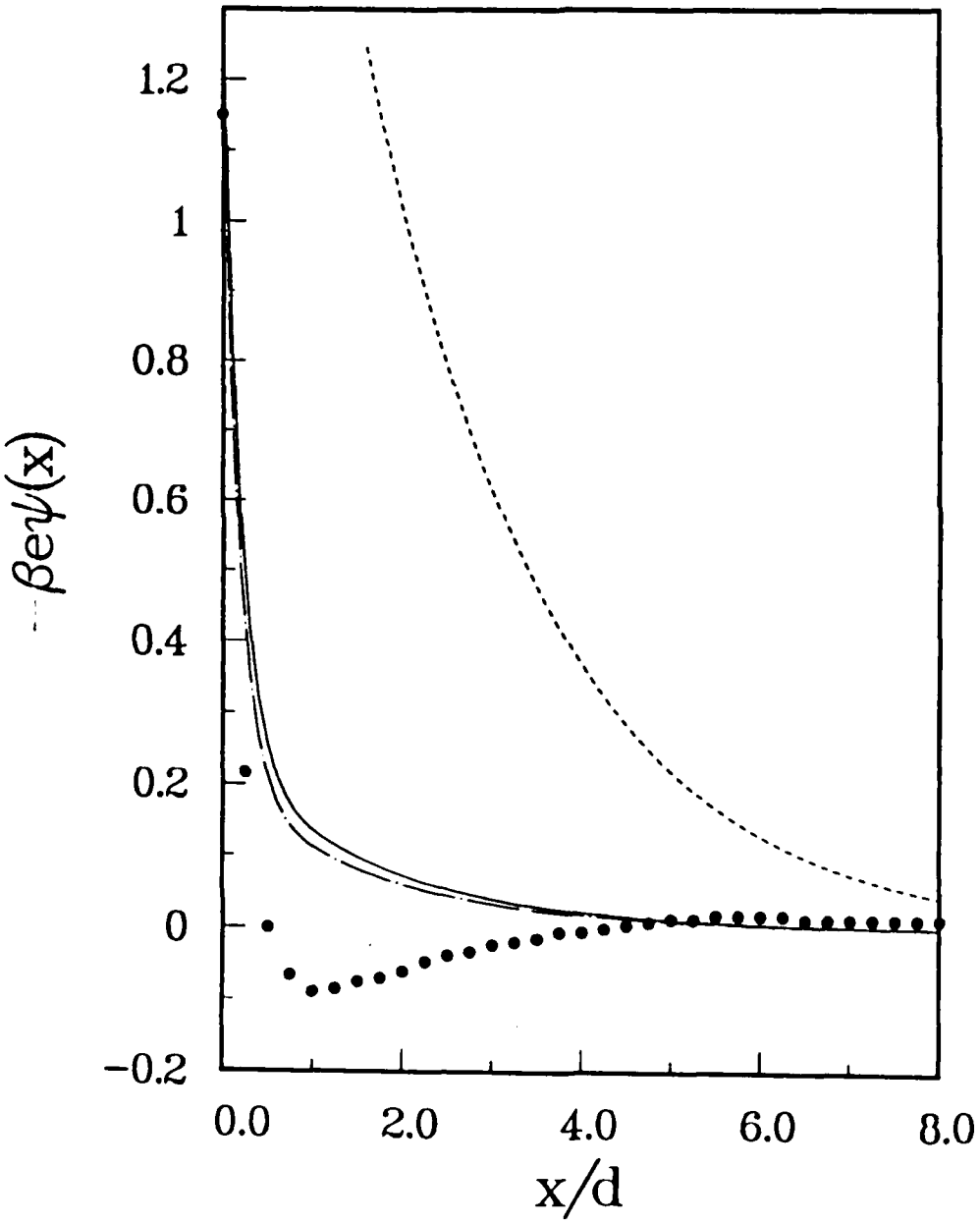

2:1
0.05 M
$\sigma^* = -0.284$

GHRM ——
MGC - - - -
MC •
T + GvdW —·—

Fig. 1

2:1

0.5 M

$\Gamma^* = -0.1704$

GHRM ——

MGC - - - - -

T + GvdW —•—

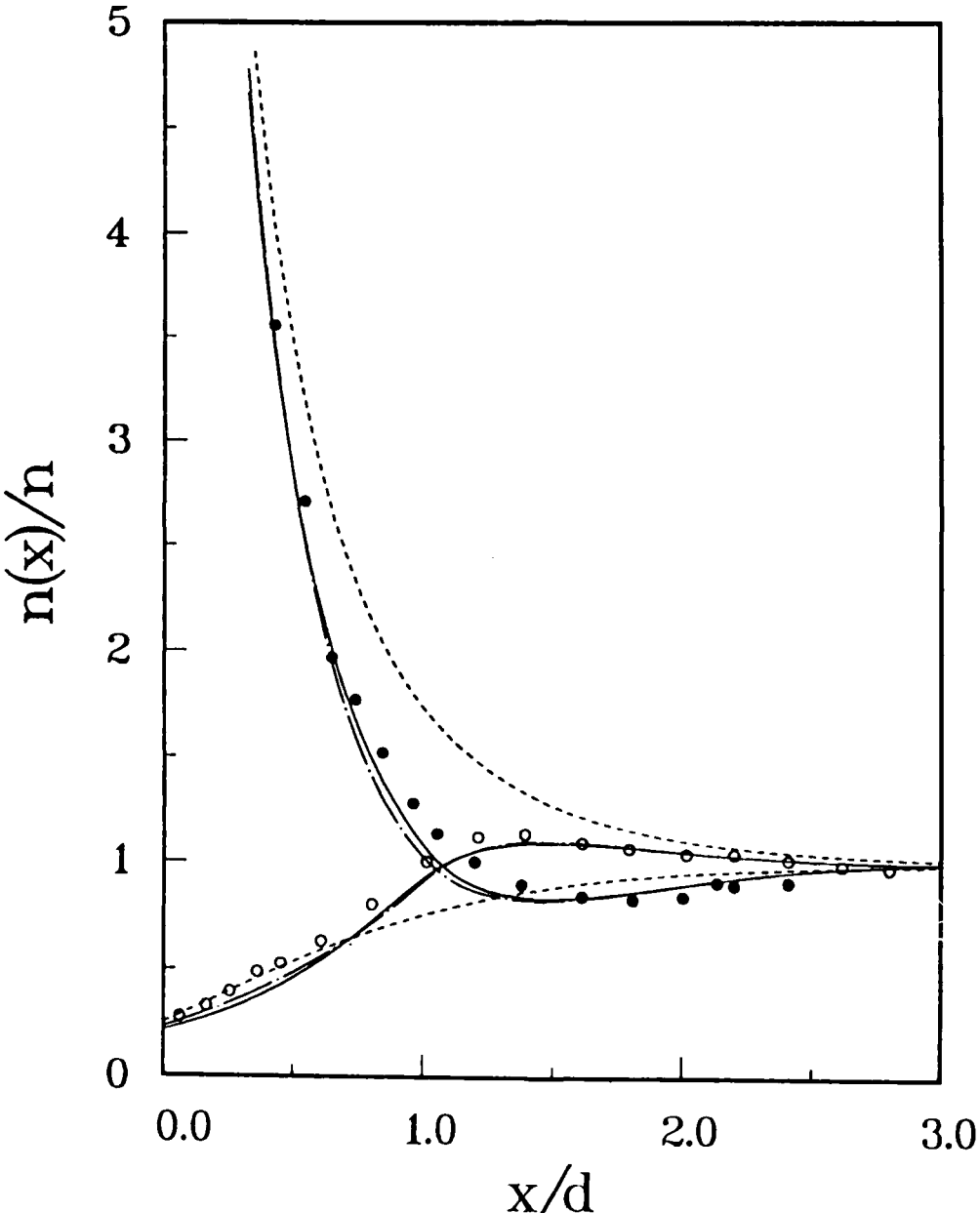

Fig. 8

2:1
c = 0.5 M
$\Gamma^* = -0.1704$

GHRM ——
MGC - - - -
T+GvdW —·—

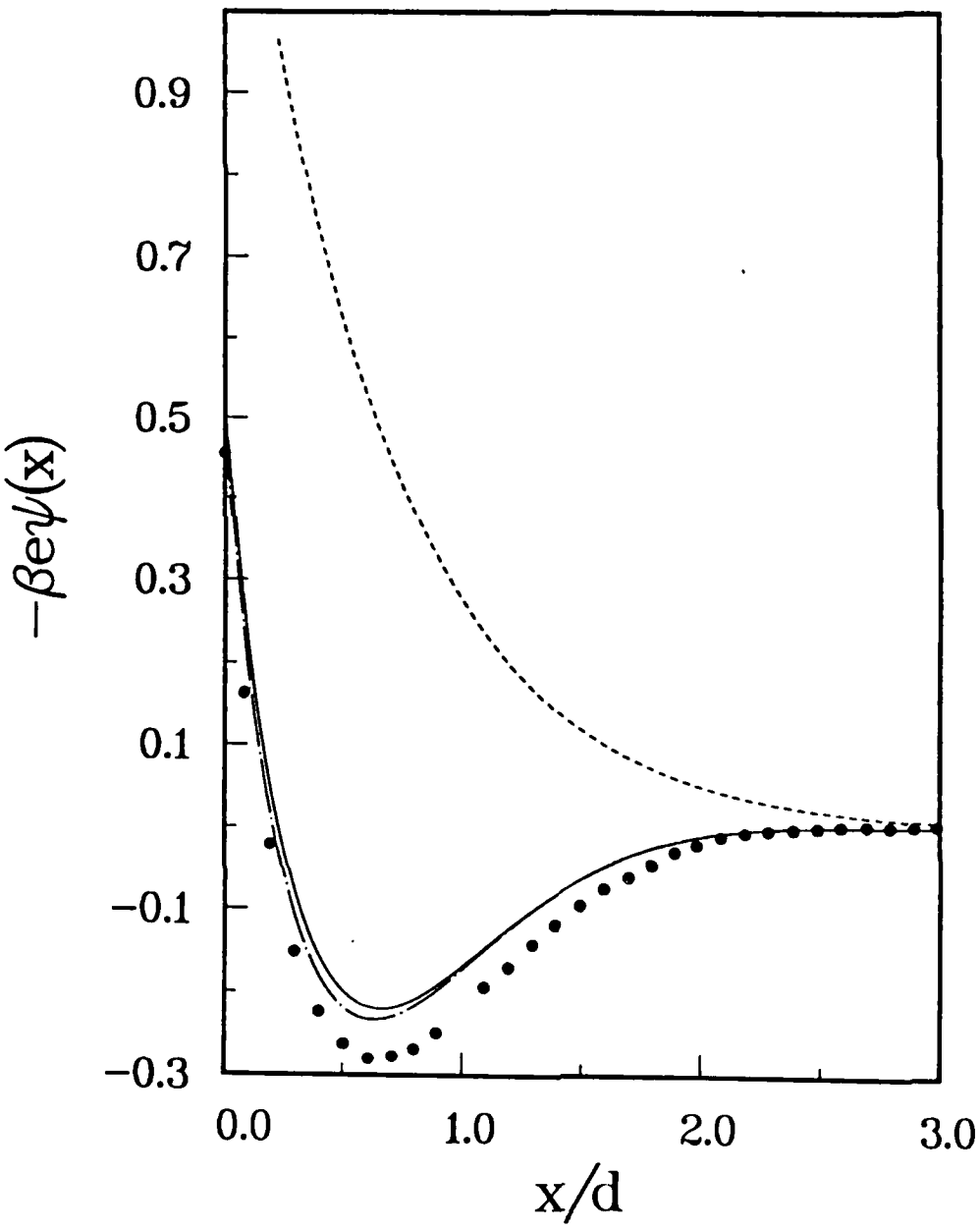

Fig. 9